

## **Thermal evolution of Vacancy defects induced in sintered UO<sub>2</sub> disks by helium implantation**

H. Labrim<sup>1</sup>, M.-F. Barthe<sup>1\*</sup>, P. Desgardin<sup>1</sup>, T. Sauvage<sup>1</sup>, G. Blondiaux<sup>1</sup>, C. Corbel<sup>2</sup> and J.P. Piron<sup>3</sup>

<sup>1</sup> *CERI - CNRS, 3A rue de la Férollerie 45071 Orléans, France*

<sup>2</sup> *Laboratoire des Solides Irradiés, Ecole polytechnique, F-91128, Palaiseau, France*

<sup>3</sup> *DEN/DEC/SESC, CEA Cadarache, 13108 Saint Paul Lez Durance, France*

\* Corresponding author : MF Barthe, Phone +33.2.38.25.54.29, Fax +33.2.38.63.02.71  
[barthe@cnrs-orleans.fr](mailto:barthe@cnrs-orleans.fr)

**Abstract :** A Slow positron beam coupled with Doppler broadening spectrometer was used to measure the low and high momentum annihilation fractions, S and W respectively as a function of positron energy in UO<sub>2</sub> disks implanted with different 1 MeV <sup>3</sup>He fluences and annealed in ArH<sub>2</sub> or in vacuum. The S(E) and W(E) behaviors indicate that for fluences in the range from 2x10<sup>14</sup> to 2x10<sup>16</sup> <sup>3</sup>He.cm<sup>-2</sup>, the vacancy defects distribution evolves with the annealing temperature in the range from 264 to 700°C under ArH<sub>2</sub>. This evolution is found to be dependent on the <sup>3</sup>He fluence implanted in the sintered UO<sub>2</sub> disks. For the lowest fluence of 2x10<sup>14</sup> <sup>3</sup>He.cm<sup>-2</sup>, the S(W) plot with positron energy as the running parameter suggests that only the concentration of vacancy defects decreases when annealing temperature increases. For the highest implantation fluences (from 5x10<sup>15</sup> to 2x10<sup>16</sup> <sup>3</sup>He.cm<sup>-2</sup>) the S(W) plot suggests that the nature of the vacancy defects changes in the annealing temperature range from 260 to 400°C. Measurements performed in implanted UO<sub>2</sub> disks annealed in vacuum have revealed a partial recovery of the vacancy defects possibly due to their recombination with mobile oxygen interstitials. The role of the Hydrogen infusion into the disk is also discussed.

**Keywords :** Slow Positron Beam, uranium dioxide, vacancy defects, helium implantation, Doppler broadening, thermal evolution, hydrogen

## Introduction

Alpha decay of actinides produces a large amount of helium in spent fuel specially in the case of MOX fuels : in MOX (burnup 47.5 GWd/tU) after 10,000 years the He amount is evaluated at  $6,700 \text{ cm}^3 \text{ STP per rod} - 4 \% \text{ He atoms/initial heavy metal atoms at/at}_{\text{HM}}$ . To foresee the physical and microstructural state of spent fuel after long term storage, it is necessary to study the behavior of helium in nuclear fuel. In CERI we are investigating the He migration process, bubble formation and He-vacancy defect interaction in  $\text{UO}_2$  using Nuclear Reaction Analysis method to determine the helium depth profile in as-implanted  $\text{UO}_2$  and positron annihilation spectroscopy to study vacancy defect properties.

The thermal recovery of radiation induced damages in  $\text{UO}_2$  has been already studied by using different techniques : Nakae et al [1] and Weber [2] have used XRD to measure the lattice parameter recovery as a function of temperature in neutron irradiated ( $9.97 \cdot 10^{17} \text{ fissions.cm}^{-3}$ ) and in decay alpha irradiated  $\text{UO}_2$  single crystals respectively. Matzke et al have studied the recovery of the damage induced in  $\text{UO}_2$  by heavy ion (Kr, Xe, Te and Cs) implantation with channeling Rutherford Backscattering [3,4]. While very few results have been published concerning the thermal recovery of vacancy defects in  $\text{UO}_2$  by using positron annihilation spectroscopy [5,6]. The annihilation characteristics (diffusion coefficient, lattice and defect lifetimes..) are not known in this  $\text{UO}_2$  matrix. This work is a part of the study we have undertaken in CERI to determine these data and the defect properties.

In this work we have used slow positron beam coupled with Doppler broadening spectroscopy (DB-SPB) to study the thermal recovery of the vacancy defects induced in the track region of 1 MeV  $^3\text{He}$  ions implanted in polished and annealed sintered  $\text{UO}_2$  disks.

## Experimental details.

Eleven disks cut from the same G set of sintered uranium (0.2 at.%  $^{235}\text{U}$ ) dioxide pellets have been used for this study. After polishing of one side, the disks were annealed at  $1700^\circ\text{C}$  in a wet  $\text{ArH}_2$  atmosphere to keep the samples at the stoichiometric composition. The mean grain size is about  $18 \mu\text{m}$  and the mean O/U ratio is  $2.0051 \pm 0.0001$  as determined by polarography. The density of the material is  $10.76 \pm 0.03 \text{ g.cm}^{-3}$ . The disks are  $300 \mu\text{m}$  thick and 8.2 mm in diameter.

Five  $\text{UO}_2$  disks have been implanted with 1 MeV  $^3\text{He}$  ions using the 3.5 MeV Van de Graaff accelerator at CERI Orléans. The implantations have been performed by focusing the beam ( $1 \times 1 \text{ mm}^2$ ) and by sweeping it over the disk surface to ensure a homogeneous fluence ( see

reference [7] for details). Five different fluences have been implanted in the range from  $2 \times 10^{14}$  to  $2 \times 10^{16}$   $^3\text{He}\cdot\text{cm}^{-2}$ . For each fluence, two or three  $\text{UO}_2$  disks have been implanted in the same run. The fluxes were fixed from  $1.6 \times 10^{11}$   $^3\text{He cm}^{-2}\cdot\text{s}^{-1}$  for the implantations at the lowest fluences and  $1.7 \times 10^{12}$   $^3\text{He cm}^{-2}\cdot\text{s}^{-1}$  for the ones performed at the highest fluences. The temperature was below to  $80^\circ\text{C}$  during implantation.

Anneals were performed in different conditions. Five 1 MeV  $^3\text{He}$  implanted  $\text{UO}_2$  disks with  $2 \times 10^{14}$ ,  $2 \times 10^{15}$ ,  $5 \times 10^{15}$ ,  $1 \times 10^{16}$  and  $2 \times 10^{16}$   $\text{cm}^{-2}$  fluences have been annealed in the same runs under reducing atmosphere, 10 vol.%  $\text{H}_2/\text{Ar}$ . The atmosphere of the furnace was purged of oxygen before annealing by  $\text{H}_2/\text{Ar}$  sweeping for 1 hour. The heating rate was approximately  $10^\circ\text{C}\cdot\text{min}^{-1}$ . The annealing lasted 1 hour except for the anneals at a temperature  $\leq 264^\circ\text{C}$  which lasted only 15 minutes. At the end of the heating,  $\text{H}_2/\text{Ar}$  was maintained in the furnace for approximately 15 hours during the cooling of the disks down to  $30^\circ\text{C}$  in order to prevent oxidation of the disk surface. The five implanted disks were annealed between every DB-SPB measurement at different temperatures in the  $164 - 700^\circ\text{C}$  range.

A sixth  $\text{UO}_2$  disk, implanted with 1 MeV  $^3\text{He}$  at a fluence of  $1 \times 10^{16}$   $\text{cm}^{-2}$  has been annealed under vacuum ( $8 \times 10^{-8}$  mbar). The  $\text{UO}_2$  disk was fixed on the temperature regulated sample holder -using a closed-cycle He cryocooler- mounted in the target chamber of the DB-SPB system. The heating and cooling rate was approximately of  $10^\circ\text{C}\cdot\text{min}^{-1}$ . In-situ annealings have been performed between DB-SPB measurements at increasing temperature from  $127$  to  $427^\circ\text{C}$  with  $100^\circ\text{C}$  step. The surface of the  $\text{UO}_2$  disks annealed in these conditions at  $427^\circ\text{C}$  have been found stoichiometric by XPS [8].

The positron-electron pair momentum distribution has been measured at 300 K by recording the Doppler broadening of the 511 keV annihilation line characterized by the low (S) and the high (W) momentum annihilation fractions in the momentum range  $(0 - |2.80|) \times 10^{-3} m_0c$  and  $(|10.61| - |26.35|) \times 10^{-3} m_0c$  respectively. To investigate the depth dependence of S and W, the curves S(E) and W(E) were recorded as a function of the positron energy E changed in 0.5 keV steps in the 0.5 to 25 keV range using a slow positron beam [9] at the CERI laboratory. The positron mean implantation depth in  $\text{UO}_2$  varies from approximately 1 nm to 670 nm in this energy range [10]. The disk B23 polished and annealed at  $1700^\circ\text{C}$  during 24 hours in humid  $\text{Ar}/\text{H}_2$  atmosphere has been measured regularly as a reference sample. In this disk, S and W values remain constant between 5 and 25 keV ( $S_{\text{B23}} = 0.3727(5)$ ;  $W_{\text{B23}} = 0.0783(2)$ )

## Results and discussion.

*As-received and As-implanted sintered  $\text{UO}_2$  disks :*

The study of the as-received and as-implanted  $\text{UO}_2$  disks has been published elsewhere [11]. The momentum distribution of annihilating electron-positron pairs has been measured by Doppler broadening spectroscopy with a slow positron beam in polished and  $1700^\circ\text{C}/24\text{h}/\text{ArH}_2$  annealed sintered  $\text{UO}_2$  disks. The as-received sintered polished and  $1700^\circ\text{C}/24\text{h}/\text{wet ArH}_2$  annealed  $\text{UO}_2$  disks have given reproducible results which are shown for one disk in Fig.1. The as-received  $\text{UO}_2$  disks have been found to be homogeneous with annihilation characteristics  $(S_{\text{ref}}, W_{\text{ref}}) = (0.371 (1), 0.079 (2))$  and a short effective diffusion length attributed to a high positron trapping rate at acceptor defects [11].

In the following only the relative values of the S and W characteristics will be given, determined as the ratios  $S/S_{\text{ref}}$  and  $W/W_{\text{ref}}$  respectively but still called S and W respectively to lighten the text.

*After implantation* with 1 MeV  $^3\text{He}$  at different fluences in the range from  $2 \times 10^{14}$  to  $1 \times 10^{17} \text{ } ^3\text{He cm}^{-2}$ , the S(E) and W(E) behaviors differ strongly from those measured in the as-received  $\text{UO}_2$  disks [11] as shown in Figure 1 for the  $1 \times 10^{16} \text{ } ^3\text{He cm}^{-2}$  fluence. The S(E) values are higher in the implanted disks than in the as-received ones where all the W(E) values are respectively lower. S is high at the surface and decreases very fast as E increases up to 1.5 or 2 keV depending on the ion fluence, then S(E) increases more or less fast, depending on the ion implanted fluence. W(E) behaves in a reverse way. From these experimental results and the ones obtained for the other fluences we have concluded that vacancy defects are detected in the  $^3\text{He}$  ion track region (0-1.5  $\mu\text{m}$  deep zone) corresponding to the thickness of the  $^3\text{He}$  implanted  $\text{UO}_2$  disk which is probed with slow positron beam. The vacancy defect distribution is heterogeneous as a function of depth, and their concentration increases with the depth. The nature of these vacancy defects is the same whatever the depth in the ion track region and whatever the ion fluence, in the explored range. Positron trapping at these track region vacancy defects has been shown to increase with the  $^3\text{He}$  fluence up to saturation from  $1 \times 10^{16} \text{ } ^3\text{He cm}^{-2}$  deepest in the track region and at  $1 \times 10^{17} \text{ } ^3\text{He cm}^{-2}$  for the whole thickness.

### **Thermal behavior of the vacancy defects induced in the track region of 1MeV $^3\text{He}$ ions**

The S(E) and W(E) positron annihilation characteristics in the  $^3\text{He}$  implanted sintered  $\text{UO}_2$  disks, annealed under  $\text{ArH}_2$ , differ strongly depending on the temperature. For all the  $^3\text{He}$  implanted fluences, the first annealing at  $164^\circ\text{C}$  during 20 minutes doesn't change anything in the S(E) and W(E) behaviour compared to the as-implanted state, as shown for  $1 \times 10^{16} \text{ } ^3\text{He cm}^{-2}$  in figure 1. After annealing at  $263^\circ\text{C}$  during 15 min, strong changes can be observed in the S(E) and W(E) behaviour. For positron energy higher than  $E_i$  in the range between 2.5 and 5 keV depending on the

$^3\text{He}$  fluence, the  $S(E)$  values are lower and the  $W(E)$  respectively higher in the  $264^\circ\text{C}/15\text{min}$  annealed disks than in the as-implanted ones. Nevertheless these values remain higher than the ones measured in the  $\text{UO}_2$  disks before implantation. Whatever the  $^3\text{He}$  fluence the  $S(E)$  and  $W(E)$  have the same general appearance as described for the  $1 \times 10^{16} \text{ } ^3\text{He cm}^{-2}$  implanted  $\text{UO}_2$  disk in the following.  $S$  has a high value at the surface and decreases very fast up to 1.5 keV, and then more slowly up to 3.5 keV. From this energy up to 6.5 keV,  $S(E)$  remains approximately constant. Finally, from 7 keV,  $S(E)$  increases again up to 25 keV (Fig 1.a).  $W(E)$  behaves in a reverse way (Fig 1.b). The  $S(W)$  plot, for positron energies above 1.5 keV, consists of only one segment of straight line, denoted  $D_{\text{imp}}$  (Fig. 1c).  $D_{\text{imp}}$  is identical to the straight line which is characteristic of annihilation at the vacancy defects induced in  $\text{UO}_2$  by  $^3\text{He}$  implantation, that we will call  $V_{\text{imp}}$  [11]. It indicates that the nature of the detected vacancy defects doesn't change after the  $264^\circ\text{C}/15\text{min}$  annealing in  $1 \times 10^{16} \text{ } ^3\text{He cm}^{-2}$  implanted  $\text{UO}_2$  disk. The  $S(E)$  increase and the  $W(E)$  decrease, when the positron energy increases, respectively indicate an heterogeneous vacancy defect distribution with a lower  $V_{\text{imp}}$  detection near the surface than deeper in the track layer.

For the annealings performed at higher temperatures, whatever the  $^3\text{He}$  fluence,  $S$  and  $W$  more or less change depending on the depth, the fluence and the annealing temperature. Nevertheless  $S$  and  $W$  always remain higher and lower than 1 respectively, indicating that total recovery of the implantation induced damage is not obtained for temperatures  $\leq 700^\circ\text{C}$ .

In Figure 2,  $S_m$  and  $W_m$  -calculated as the mean values of the three consecutive  $S(E)$  and respectively  $W(E)$  points around 24.5 keV- have been plotted as a function of the annealing temperature, fixed between room temperature and  $700^\circ\text{C}$ . For all  $^3\text{He}$  fluences,  $S_m$  and  $W_m$  begin to decrease and to increase for  $264^\circ\text{C}/15\text{min}$  annealing respectively. For annealing performed at temperatures  $\geq 264^\circ\text{C}$ , the  $S_m$ ,  $W_m$  behaviours depend on the  $^3\text{He}$  fluence. For the lowest fluence ( $2 \times 10^{14} \text{ } ^3\text{He.cm}^{-2}$ ),  $S_m$  and  $W_m$  remain approximately constant when the temperature increases up to  $700^\circ\text{C}$ . These ( $S_m$ ,  $W_m$ ) plateaux values are very closed to the ones measured into the as-received polished and  $1700^\circ\text{C}/24\text{h}/\text{ArH}_2$  annealed  $\text{UO}_2$  disks but remain higher and respectively lower. It indicates that the defect distribution is different after implantation and annealing from in the as-received state, it could be due to the decrease in the concentration of negatively charged traps detected in the as-received  $\text{UO}_2$  disks.

For the  $^3\text{He}$  fluences  $\geq 2 \times 10^{15} \text{ cm}^{-2}$   $S_m$  and  $W_m$  go on to decrease and to increase respectively when  $300^\circ\text{C}/1\text{h}$  annealing is performed. This variation is emphasized dramatically for the highest  $^3\text{He}$  fluences  $\geq 1 \times 10^{16} \text{ cm}^{-2}$ . Then  $S_m$  and  $W_m$  remain approximately constant after  $400^\circ\text{C}/1\text{h}$  annealing for all the fluences indicating that as in the lowest  $^3\text{He}$  fluence implanted  $\text{UO}_2$ , the vacancy defect distribution doesn't evolve for heating between  $300^\circ\text{C}$  and  $400^\circ\text{C}$ . From  $500^\circ\text{C}$ ,

$W_m$  begins to decrease up to 600°C and remains approximately constant after 700°C/1h annealing. In the same temperature range,  $S_m$  remains constant for  $^3\text{He}$  fluence  $< 1 \times 10^{16} \text{ cm}^{-2}$  and slightly increases for the highest fluences. The major increase in  $W_m$  observed for annealing at temperatures around 300°C is correlated with the change of slope that is clearly displayed in figure 3 where the  $(S_m, W_m)$  points have been plotted with annealing temperature as the running parameter for all the  $^3\text{He}$  fluences. Except after the anneals performed at 300°C and 400°C for all the fluences and at 264°C for the lowest fluences  $\leq 2 \times 10^{15} \text{ cm}^{-2}$ , the majority of  $(S_m, W_m)$  points are aligned on the same straight line  $D_{\text{imp}}$ .  $D_{\text{imp}}$  goes through the  $(S_{\text{ref}}, W_{\text{ref}})$  point and through all the  $(S_m, W_m)$  points measured in the as-implanted  $\text{UO}_2$  disks. This  $D_{\text{imp}}$  straight line is identical to the one which has been found to characterize the vacancy defects  $V_{\text{imp}}$  induced in the ion track region by 1 MeV  $^3\text{He}$  implantation in  $\text{UO}_2$  [11]. The  $(S_m, W_m)$  points measured after the anneals performed at 300°C and 400°C for all the fluences and at 264°C for the lowest fluences  $\leq 2 \times 10^{15} \text{ cm}^{-2}$  are aligned on or seem to go to join a second straight line  $D_H$  which goes through the  $(S_{\text{ref}}, W_{\text{ref}})$  point but has a higher slope than  $D_{\text{imp}}$ . It indicates that after annealing at 300°C the positrons are trapped at vacancy defects called  $V_H$ , and which have a different nature compare to  $V_{\text{imp}}$ .  $V_H$  with an identical trapping rate are still detected after the 400°C/1h heating. This change in nature is also clearly shown in figure 1c for the  $1 \times 10^{16} \text{ } ^3\text{He cm}^{-2}$  implanted  $\text{UO}_2$  disk, annealed at 400°C/1h. The  $S(W)$  plot, for positron energies above 4 keV, consists of only one agglomerate of points, and its barycentre is located above the segment of straight line  $D_{\text{imp}}$ .

When the annealing temperature reaches 500°C, the  $(S_m, W_m)$  points for all the fluences are again aligned on the  $D_{\text{imp}}$  straight line (Fig. 3 and 1c) indicating that the positrons no longer see  $V_H$  defects, and  $V_{\text{imp}}$  are again detected with a lower trapping rate than before any annealing. This second  $D_H$   $(S, W)$  line is not observed for the  $\text{UO}_2$  disk implanted with 1MeV  $^3\text{He}$  at  $1 \times 10^{16} \text{ cm}^{-2}$  fluence and annealed under vacuum in the temperature range from 127°C up to 427°C (figure 4). These  $V_H$  defects seem to be revealed when the anneals are performed in a hydrogenated atmosphere ( $\text{ArH}_2$ ). It is also clear that the low momentum fraction  $S$  and the high momentum fraction  $W$  decreases and increases respectively after heating under vacuum, but the  $(S, W)$  points remain on the  $D_{\text{imp}}$  straight line. It indicates that only the trapping rate at  $V_{\text{imp}}$  vacancy defects, induced in the track region by He implantation, is reduced under vacuum annealing from 227°C up to 427°C. It suggests that in this temperature range some recombinations of implantation induced vacancy defects begin to occur and operate in the total temperature range from 227°C up to 427°C. These partial recovery could be due to the Oxygen interstitials which have been found to become mobile from about 200°C [12].

When annealing is performed under ArH<sub>2</sub> atmosphere the changes in S and W are much more pronounced, and a stabilized value of trapping at V<sub>H</sub> defects is already obtained at 300°C. It suggests that the O<sub>i</sub> related recombinations are not the only process to be considered, but compete with another phenomenon which can be related to H<sub>2</sub> infusion in the UO<sub>2</sub> samples. Indeed Wheeler et al have determined the H diffusion coefficient  $D_{Hyd}$  in UO<sub>2</sub> in the temperature range from 500 to 1000°C :  $D_{Hyd} [\text{cm}^2/\text{s}] = 0.037 \times \exp(-14.3 [\text{kcal mol}^{-1}]/RT [\text{K}])$  [13]. Extrapolating these data for 300°C, the diffusion length of about 300 μm can be expected for 1 hour annealing, indicating that hydrogen can go through the full thickness of the 300 μm thick disk during annealing. We have also shown by using NRA that H<sub>2</sub> infuses in UO<sub>2</sub> for 400°C/3h/ ArH<sub>2</sub> annealing [14]. The consequences of the H<sub>2</sub> infusion in the implanted disks can be of two types. The first one which can be considered is the decoration of the defects created by He implantation with hydrogen. This decoration may change the chemical environment that is seen by the positron trapped at these defects. It should lead to a change in the W values but should not change the S values too much if no relaxation occurs due to the H decoration. The second possible consequence of the H<sub>2</sub> infusion could be the hydrogen trapping at vacancy defects induced by the He implantation leading to a decrease of positron trapping at these defects. If only one type of vacancy defect is detected in the track region of the He implanted UO<sub>2</sub> disks, it should imply the decrease of the low momentum annihilation fraction S and the increase of the high momentum annihilation fraction W, but not the slope change that has been observed for the annealing performed under ArH<sub>2</sub> in the temperature range of 300°C to 400°C. It suggests that several vacancy defects are detected after He implantation and one of them is more efficient at trapping H<sub>2</sub> than the other one.

The positron trapping at these H related defects V<sub>H</sub> decreases while the one at the vacancy defects V<sub>imp</sub> induced in the track region by He implantation increases when annealing is performed at temperature higher than 500°C. It suggests that the hydrogen decoration or trapping begins to become less efficient when the annealing temperature becomes higher than 500°C.

## Summary

The momentum distribution of annihilating electron-positron pairs has been measured by Doppler broadening spectroscopy with a slow positron beam in polished and 1700°C/24h/ArH<sub>2</sub> annealed sintered UO<sub>2</sub> disks after implantation and annealing in ArH<sub>2</sub> or in vacuum. The distribution of the vacancy defects created in the track region of the 1MeV <sup>3</sup>He ions has been found to change with the annealing conditions. The trapping at these vacancy defects has been found to decrease for annealing performed in vacuum. It suggests a partial recovery observed from 227°C/1h and possibly attributed to the recombination with the mobile oxygen interstitials. When annealing has

been performed in ArH<sub>2</sub>, the trapping reduction at the implantation induced vacancy defects is more pronounced indicating the influence of the Hydrogen infusion in the UO<sub>2</sub> disks. The Hydrogen decoration of the vacancy defects induced by He implantation or its trapping at some of these defects have been suggested to explain the thermal evolution of the vacancy defects distribution .

### Acknowledgements

The authors are grateful to the French electrical utility Électricité de France (EDF) and the Research Program on the long term Evolution of Spent Fuel waste Packages of the CEA (PRECCI) for their financial support.

### References

- [1] N. Nakae, Y. Iwata, and T. Kirihara, *Journal of Nuclear Materials* **80**, 314 (1979).
- [2] W. J. Weber, *Journal of Nuclear Materials* **114**, 213 (1983).
- [3] H. Matzke and A. Turos, *Nuclear Instruments & Methods in Physics Research, Section B Beam Interactions with Materials and Atoms* **46**, 117 (1990).
- [4] H. Matzke and A. Turos, *Journal of Nuclear Materials* **188**, 285 (1992).
- [5] H. E. Evans, J. H. Evans, P. Rice-Evans, et al., *Journal of Nuclear Materials* **199**, 79 (1992).
- [6] M.-F. Barthe, S. Guilbert, H. Labrim, P. Desgardin, T. Sauvage, G. Blondiaux, G. Carlot, P. Garcia and J.P. Piron, *Materials Science Forum*, Vols 445-446, 2004, p. 48
- [7] S. Guilbert, T. Sauvage, P. Garcia, et al., *Journal of Nuclear Materials* **327**, 88 (2004).
- [8] F. Miserque CEA Report (2004)
- [9] P. Desgardin, L. Liskay, M.-F. Barthe, et al: *Mater. Sci. Forum* Vol.363-365 (2001), p. 523.
- [10] E. Soininen, J. Mäkinen, D. Beyer and P. Hautojärvi, *Phys. Rev. B* **46** (1992), p. 13104
- [11] MF Barthe, H. Labrim, P. Desgardin, T. Sauvage, C. Corbel, G. Blondiaux and J.P. Piron submitted at the SLOPOS10 workshop, to be published
- [12] A. Turos, H. Matzke, and S. Kwiatkowski, *Physical Review Letters* **65**, 1215 (1990).
- [13] V. J. Wheeler, *J. Nucl. Mat.*, **40**, (1971) 189.
- [14] H. Labrim, M.-F. Barthe, T. Sauvage, P. Desgardin, G. Blondiaux , C. Corbel, F. Miserque and J.P. Piron, to be published in NIMB

## Figure Captions

**Figure 1:** Relative low momentum annihilation fraction  $S/S_{\text{ref}}$  and relative high momentum annihilation fraction  $W/W_{\text{ref}}$  as a function of positron energy (a,b respectively) and  $S/S_{\text{ref}}$  as a function of  $W/W_{\text{ref}}$  (c) in  $\text{UO}_2$  disks before (+) and after 1 MeV  $^3\text{He}$  implantation at the  $1 \times 10^{16} \text{ cm}^{-2}$  fluence (★) and after annealing in  $\text{ArH}_2$  at different temperatures ( $\triangle$  164°C,  $\square$  263°C,  $\blacktriangledown$  400°C and  $\diamond$  700°C).

**Figure 2:** Mean values of low momentum fraction  $S_m$  (2a) and high momentum fraction  $W_m$  (2b) at positron energy of 24.5 keV as a function of annealing temperature for the  $\text{UO}_2$  disks implanted with 1 MeV  $^3\text{He}$  at 5 different fluences from  $2 \times 10^{14}$  up to  $2 \times 10^{16} \text{ cm}^{-2}$  and annealed in  $\text{ArH}_2$  atmosphere.

**Figure 3:** Low momentum fraction mean value  $S_m$  as a function of high momentum fraction mean value  $W_m$  at positron energy of 24.5 keV for the  $\text{UO}_2$  disks implanted with 1 MeV  $^3\text{He}$  at 5 different fluences from  $2 \times 10^{14}$  up to  $2 \times 10^{16} \text{ cm}^{-2}$  and annealed in  $\text{ArH}_2$  atmosphere at different temperatures in the range from 164°C up to 700°C.

**Figure 4:** Low momentum fraction mean value  $S_m$  as a function of high momentum fraction mean value  $W_m$  at positron energy of 24.5 keV for the  $\text{UO}_2$  disks implanted with 1 MeV  $^3\text{He}$  at  $1 \times 10^{16} \text{ cm}^{-2}$  fluence and annealed in  $\text{ArH}_2$  atmosphere or in vacuum at different temperatures in the range from 164°C up to 700°C.



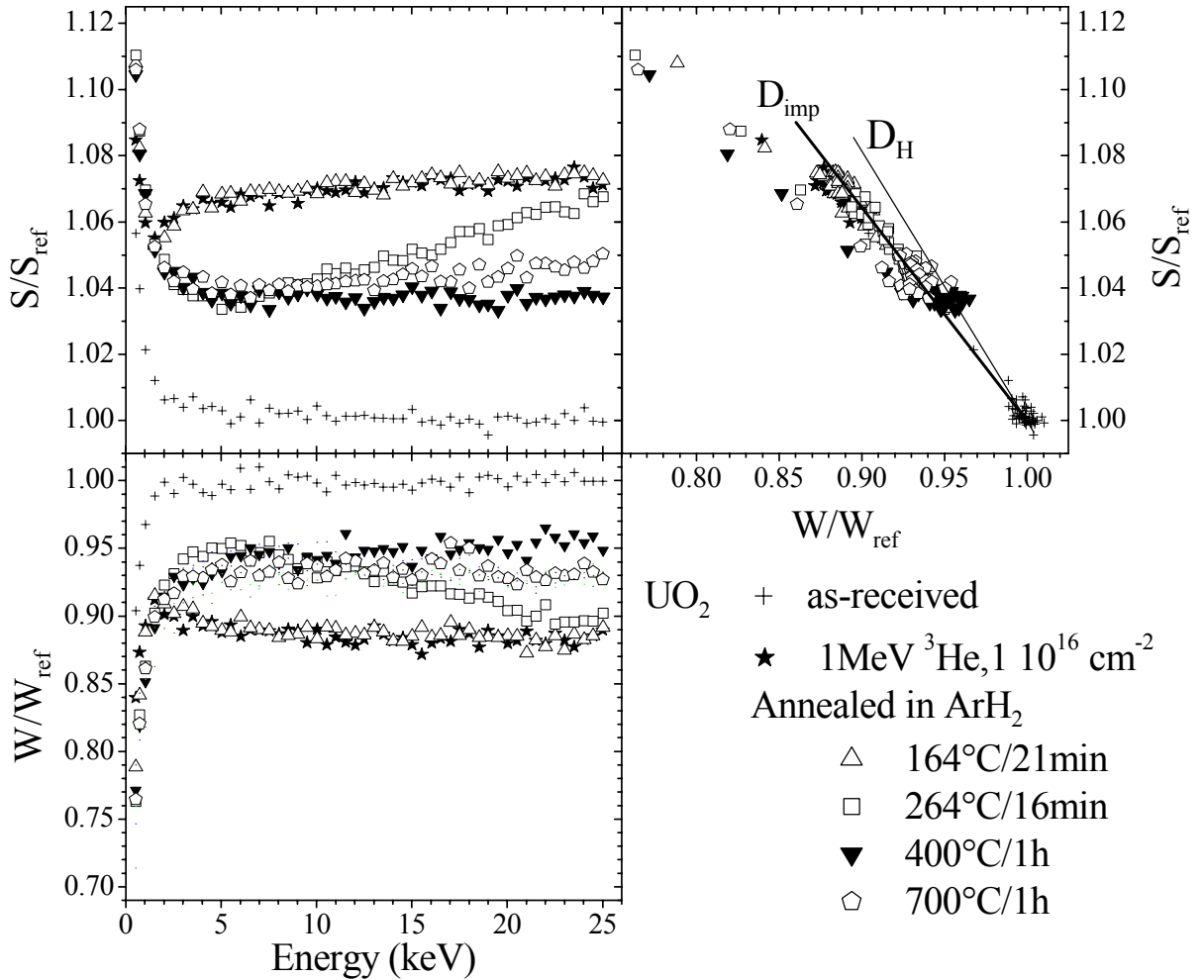


**Figure 1:** Relative low momentum annihilation fraction  $S/S_{ref}$  and relative high momentum annihilation fraction  $W/W_{ref}$  as a function of positron energy (a,b respectively) and  $S/S_{ref}$  as a function of  $W/W_{ref}$  (c) in  $UO_2$  disks before (+) and after 1 MeV  $^3He$  implantation at the  $1 \times 10^{16} cm^{-2}$  fluence (★) and after annealing in  $ArH_2$  at different temperatures ( $\triangle$  164°C,  $\square$  263°C,  $\blacktriangledown$  400°C and  $\diamond$  700°C).

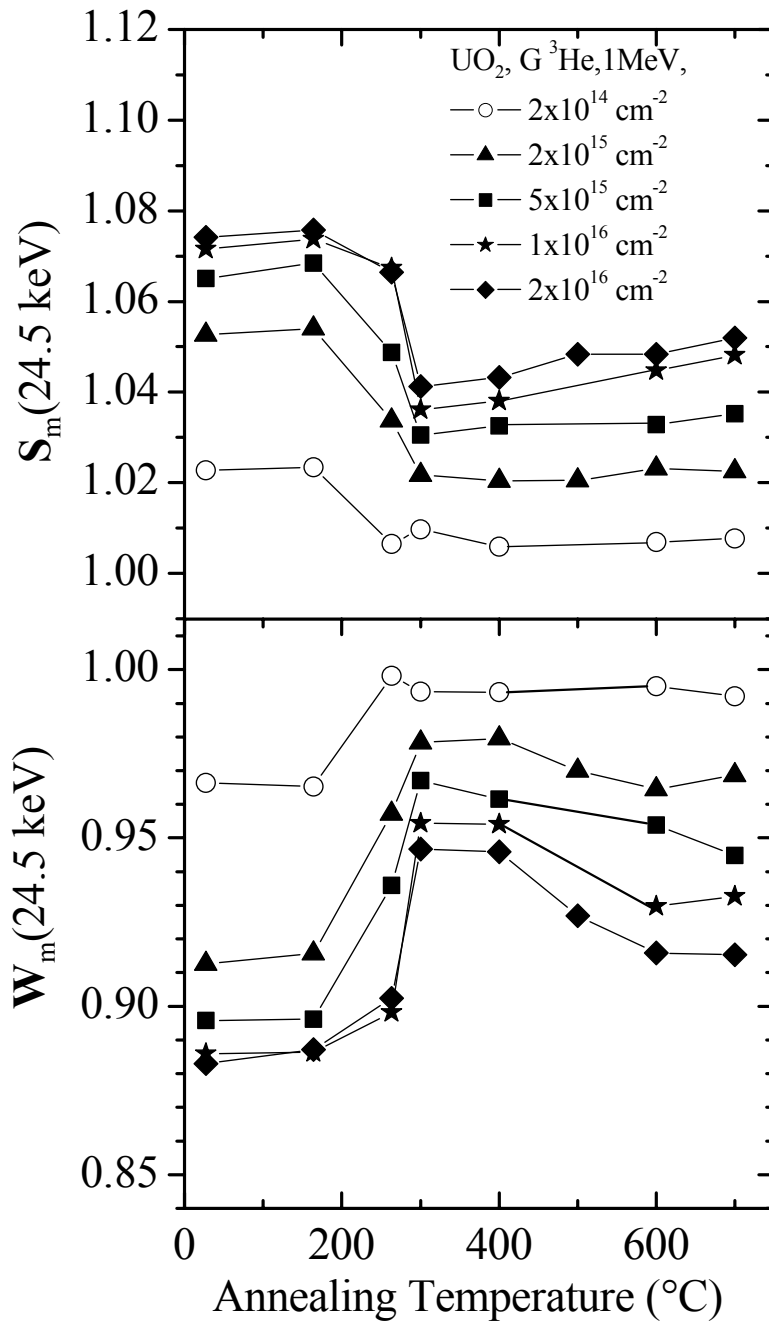


**Figure 2:** Mean values of low momentum fraction  $S_m$  (2a) and high momentum fraction  $W_m$  (2b) at positron energy of 24.5 keV as a function of annealing temperature for the  $\text{UO}_2$  disks implanted with 1 MeV  ${}^3\text{He}$  at 5 different fluences from  $2 \times 10^{14}$  up to  $2 \times 10^{16} \text{ cm}^{-2}$  and annealed in  $\text{ArH}_2$  atmosphere.

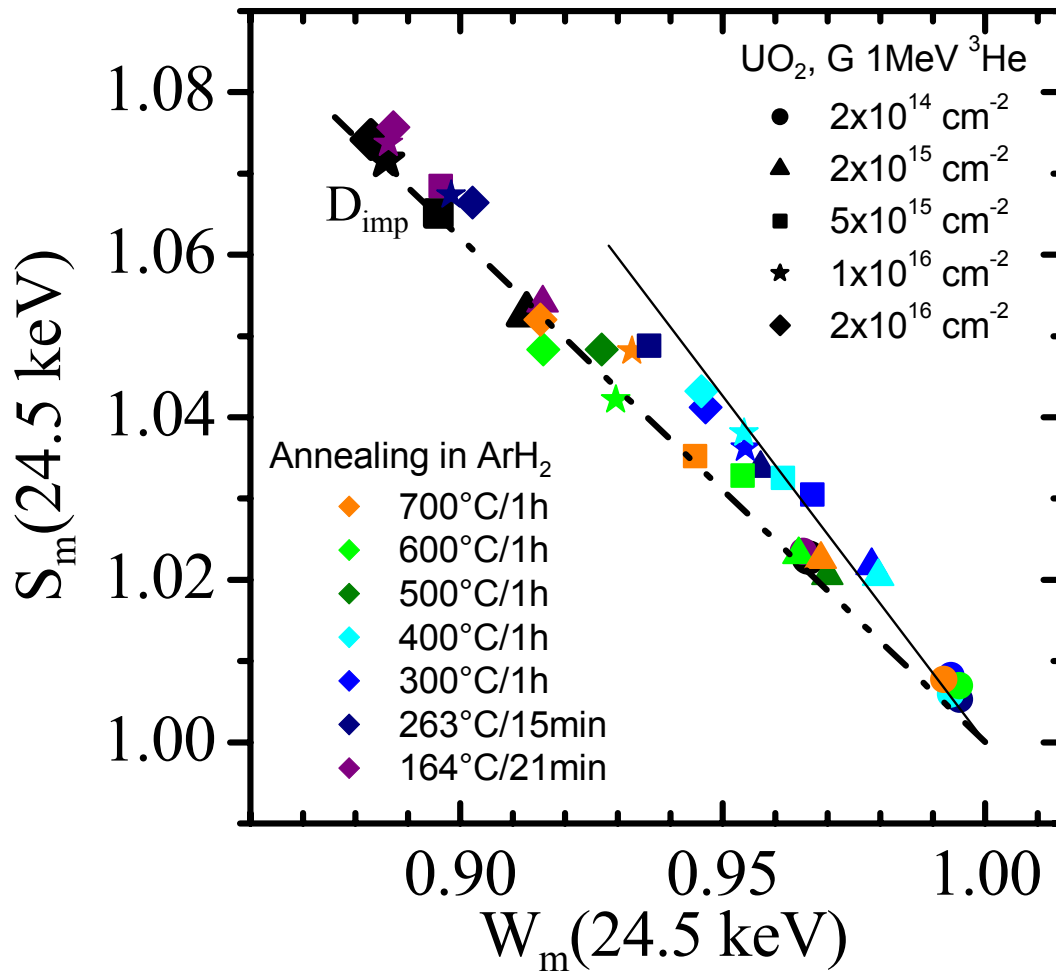


**Figure 3:** Low momentum fraction mean value  $S_m$  as a function of high momentum fraction mean value  $W_m$  at positron energy of 24.5 keV for the  $\text{UO}_2$  disks implanted with 1 MeV  $^3\text{He}$  at 5 different fluences from  $2 \times 10^{14}$  up to  $2 \times 10^{16} \text{ cm}^{-2}$  and annealed in  $\text{ArH}_2$  atmosphere at different temperatures in the range from  $164^\circ\text{C}$  up to  $700^\circ\text{C}$ .

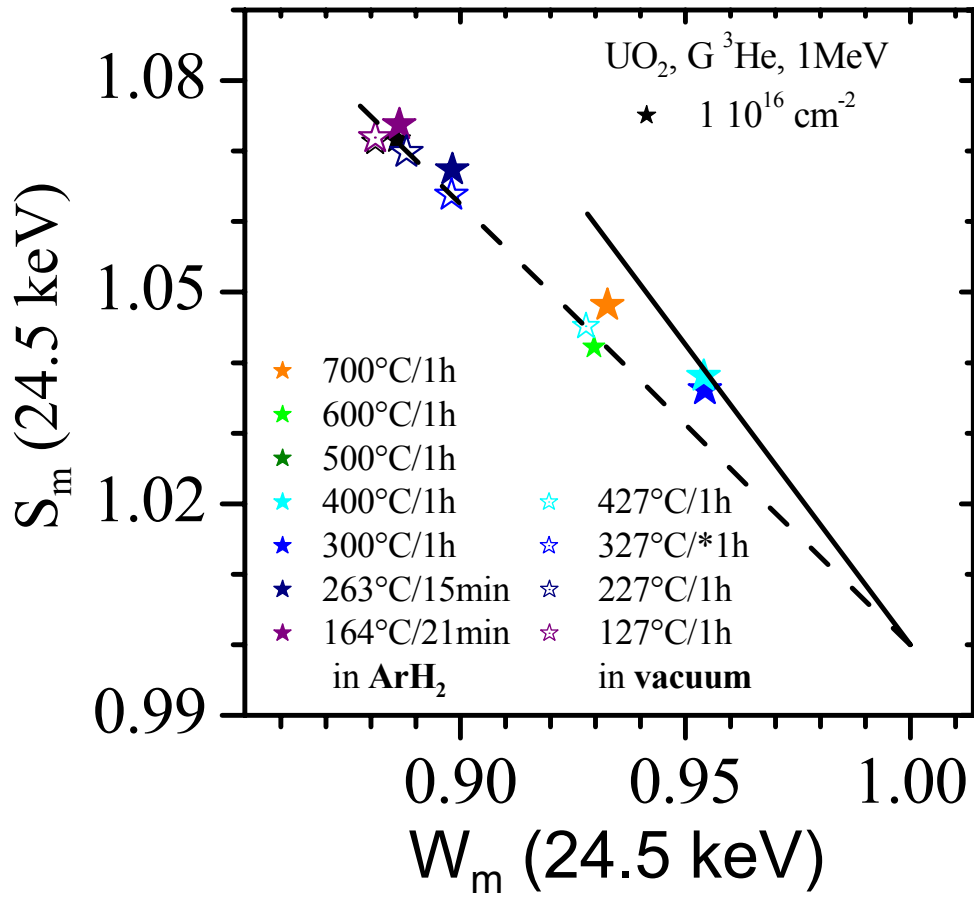


**Figure 4:** Low momentum fraction mean value  $S_m$  as a function of high momentum fraction mean value  $W_m$  at positron energy of 24.5 keV for the  $UO_2$  disks implanted with 1 MeV  $^3\text{He}$  at  $1 \times 10^{16} \text{ cm}^{-2}$  fluence and annealed in  $\text{ArH}_2$  atmosphere or in vacuum at different temperatures in the range from 164°C up to 700°C.

**References :**

---

- [1] N. Nakae, Y. Iwata, and T. Kirihara, *Journal of Nuclear Materials* **80**, 314 (1979).
- [2] W. J. Weber, *Journal of Nuclear Materials* **114**, 213 (1983).
- [3] H. Matzke and A. Turos, *Nuclear Instruments & Methods in Physics Research, Section B Beam Interactions with Materials and Atoms* **46**, 117 (1990).
- [4] H. Matzke and A. Turos, *Journal of Nuclear Materials* **188**, 285 (1992).
- [5] H. E. Evans, J. H. Evans, P. Rice-Evans, et al., *Journal of Nuclear Materials* **199**, 79 (1992).
- [6] M.-F. Barthe, S. Guilbert, H. Labrim, P. Desgardin, T. Sauvage, G. Blondiaux, G. Carlot, P. Garcia and J.P. Piron, *Materials Science Forum*, Vols 445-446, 2004, p. 48
- [7] S. Guilbert, T. Sauvage, P. Garcia, et al., *Journal of Nuclear Materials* **327**, 88 (2004).
- [8] F. Miserque CEA Report (2004)
- [9] P. Desgardin, L. Liskay, M.-F. Barthe, et al: *Mater. Sci. Forum* Vol.363-365 (2001), p. 523.
- [10] E. Soininen, J. Mäkinen, D. Beyer and P. Hautojärvi, *Phys. Rev. B* **46** (1992), p. 13104
- [11] MF Barthe, H. Labrim, P. Desgardin, T. Sauvage, C. Corbel, G. Blondiaux and J.P. Piron submitted at the SLOPOS10 workshop, to be published
- [12] A. Turos, H. Matzke, and S. Kwiatkowski, *Physical Review Letters* **65**, 1215 (1990).
- [13] V. J. Wheeler, *J. Nucl. Mat.*, **40**, (1971) 189.
- [14] H. Labrim, M.-F. Barthe, T. Sauvage, P. Desgardin, G. Blondiaux, C. Corbel, F. Miserque and J.P. Piron, to be published in NIMB